Jupiter Radiation Belt Engineering Model*

Neil Divine
Jet Propulsion Laboratory

On the basis of earth observations of the HF and UHF radio emission generated near Jupiter, the presence of energetic charged particles trapped in the planet's dipole magnetic field has been inferred. For electrons, energies of the order of 10 MeV and peak fluxes of the order of 10^7 cm^{-2} s^{-1} can be derived from the data for equatorial regions about two planetary radii from the dipole. Energetic protons and lower-energy electrons and protons are also expected, but the limited data require that their fluxes be based on theory or earth analogy. Because descriptions available in the literature suggest large associated uncertainties, both nominal and limiting models for the charged-particle populations of Jupiter's belts are derived. These new engineering models describe electron and proton fluxes and their distributions in energy and position in forms suitable as space vehicle design criteria.

In the planning of missions to encounter the planet Jupiter both spacecraft design considerations and trajectory selection may be strongly affected by our understanding of the charged-particle environment trapped in Jupiter's magnetic field. These energetic electrons, and possibly protons, could be hazardous for spacecraft electronics and other sensitive subsystems. The presence of relativistic electrons has been inferred from analyses of Jupiter's radio emission. The extensive literature in this field has been reviewed recently by Carr and Gulkis (ref. 1) and by Warwick (ref. 2), from which the following brief summary is adapted.

RADIO DATA

The HF radiation, at wavelengths longer than about 7 m, is sporadic; the probability that it be observable is correlated with the sub-earth longitude on Jupiter and with the Jovicentric longitude of the first Galilean satellite, Io. The radiation's characteristic patterns in time and frequency coordinates permit conclusions to be drawn about the strength and configuration of Jupiter's magnetic field, although controversy surrounds many features of such interpretations. Nevertheless, the upper limit shown in figure 1 near 40 MHz for the radiofrequency in bursts reaching the earth implies a magnetic field strength of 14 G somewhere just above Jupiter's atmosphere, following the commonly accepted argument that the burst mechanism yields radiation at the local electron gyrofrequency. Thus, a magnetic dipole moment near 4×10^{30} G-cm^3, considerably stronger than the earth's, is implied for Jupiter. The dipole is probably centered on Jupiter (although displacements up to 0.7 radii south have been proposed; ref. 2), and inclined about 10 deg to Jupiter's axis. The interaction of this dipole with the solar wind leads us to anticipate a large magnetosphere, whose minimum extent (in the sunward direction) is about 50 Jupiter radii (ref. 1).

At wavelengths less than or near a few centimeters the UHF component shown in figure 1 is dominated by thermal emission from the disk, which need not be further discussed here. At wavelengths up to about 100 cm a non-thermal component is indicated on figure 1, having a flux density with very little dependence on time and frequency (generally less than 30%). Numerous characteristics indicate that this radiation is synchrotron radiation from relativistic electrons contained by Jupiter's magnetic field. Strong support for this hypothesis is provided by the radio brightness temperature contour maps obtained by aperture synthesis at 10.6 and 21 cm by Berge (ref. 3) and Branson (ref. 4). Most of this radiation is produced noticeably away from the disk of the planet, in a region elongated roughly parallel to the equator. In addition, up to 30% east-west linear polarization is observed. These characteristics, plus the beaming inferred from the flux density variations, confirm the synchrotron mechanism, and imply that the relativistic electrons are most abundant near Jupiter's magnetic equator. The models in the following sections have been derived from these data for use as NASA space vehicle design criteria, and are discussed more fully in ref. 5.

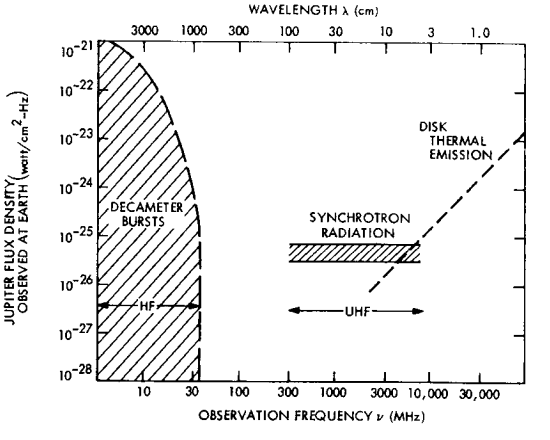

Figure 1. Schematic radio spectrum of Jupiter, adapted from Carr and Gulkis (ref. 1)

*This paper presents the results of one phase of research carried out at the Jet Propulsion Laboratory, California Institute of Technology, under Contract No. NAS 7-100, sponsored by the National Aeronautics and Space Administration.

RELATIVISTIC ELECTRONS

If the strength of the magnetic field at the UHF flux peak and the observed bandwidth are known, the characteristic electron energy can be derived from numerical formulas which summarize the results of synchrotron emission theory. As some of the required data are uncertain, only the order of magnitude of the electron energy near the UHF flux peaks has been evaluated at about 10 MeV (ref. 1). If a reasonable distribution of the source contributions along the line of sight is taken, the synchrotron theory also permits the local electron flux to be derived from the observed intensity. This can be done for the source as a whole, or in detail so that the distribution of electron flux with position is obtained.

For Jupiter's equatorial plane, figure 2 shows the results of several such derivations; the differences among them result from the application of various combinations of reasonable assumptions required in the analysis. The result credited to Carr and Gulkis (ref. 1) is simply an order-of-magnitude estimate, in which a flux of 10^7 relativistic electrons/cm^2 s occurs in a broad region of space surrounding Jupiter. The models of Branson (ref. 4) and Luthey and Beard (ref. 6) are based on the observations alone, but the poor resolution of the data is reflected by the lack of detail in their results. The model of Eggen (ref. 7) is based on earth analogy as well as on the data, but the details of this model result from the analogy and are unrealistic. The model described by Warwick (ref. 2) is based on both the data and on a physical mechanism for the population of Jupiter's radiation belts. That mechanism is the L-shell diffusion of solar wind electrons which have penetrated the outer boundary of the magnetosphere, and predicts a position distribution proportional to L^{-4} away from the observed peak within two radii of the planet.

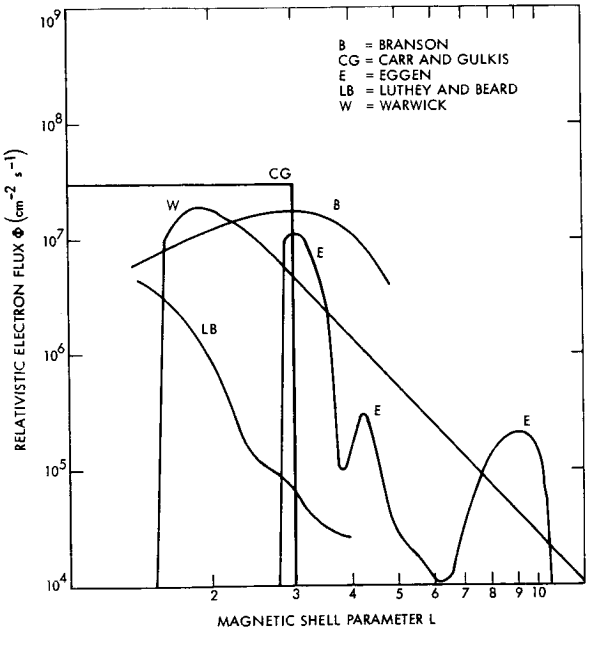

Figure 2. Flux Φ of relativistic electrons as functions of distance L from the dipole (in Jupiter radii) in the plane of the magnetic equator, as derived by the authors listed

The new engineering models reported here are plotted in figure 3 to the same scale as in figure 2, and it is intended that they bracket most of the conclusions of the authors cited above. In the figure, the central line represents the nominal values and the shaded area indicates the range of the models. In particular, the nominal model resembles the L-shell diffusion model by Warwick (ref. 2), because it was felt that the successful application of such a model to the earth's outer belt protons (ref. 8) warranted its application to Jupiter as well. For simplicity in application it is flat within 2 radii of Jupiter's dipole and proportional to L^{-4} elsewhere. The limiting models in figure 3 imply uncertainty factors of 3 at the flux peak, and larger ones elsewhere, reflecting the insecurity in the numerical details of the derivation from the limited data available.

In addition to the radial dependence just discussed, the concentration of the radiation near Jupiter's magnetic equator implies that the flux depends strongly on latitude ϕ. The engineering models include a factor proportional to $\exp(-\phi^2/10^3)$ for ϕ in degrees; this dependence cuts off near latitude 30° in a manner consistent with the brief latitude analysis presented by Warwick (ref. 2).

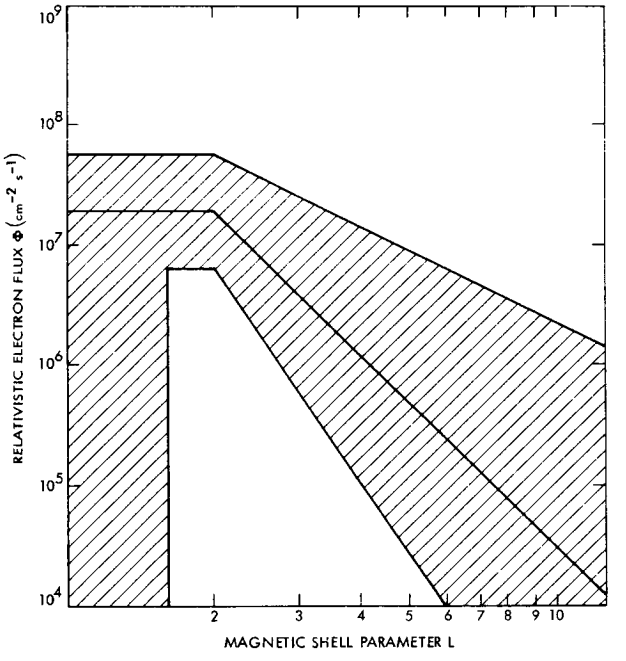

Figure 3. Flux Φ of relativistic electrons in the engineering models (same scales as fig. 2)

The electron energies, derived from the field strength and bandwidth, are near 10 MeV, but there is considerable uncertainty associated with all quantities involved. In order to achieve consistency with the features of the model adapted above from Warwick (ref. 2), the engineering models display characteristic electron energies $E_0 = 6.2 \times 3^{\pm 1}$ MeV at the flux peak, and proportional to $L^{-3\pm 2}$ elsewhere (a typical L-shell

diffusion theory dependence). Based on the synchrotron theory alone, a monoenergetic electron population would suffice to explain the observations. Nevertheless, such a distribution is probably unrealistic. The data apparently require that few low-energy electrons (ref. 9), and that few electrons above 30 MeV (ref. 4), exist near the flux peak. The differential energy distribution ($d\Phi/dE$) proportional to $(E/E_0)\exp(-E/E_0)$ is adopted for engineering purposes, because it is one of the simplest which is nearly monoenergetic (at the characteristic energy E_0) and contains an exponential term that resembles one for the earth's belts.

ENERGETIC PROTONS

There are no Jupiter data from which proton fluxes may reliably be inferred. The few published models (refs. 2, 6, 7, 10, and 11) proceed from various assumptions and derive widely divergent proton energy and flux values. Apparently the most physical discussion among the above, that of Warwick (ref. 2), applies the L-shell diffusion mechanism cited for the electrons to the trapping of solar wind protons within Jupiter's magnetosphere. The result is a number density everywhere equal to that of the electrons and identical energy characteristics, where E_0 = 29 MeV at the flux peak. In the absence of relevant data and theoretical predictions of equilibria among complex source and loss mechanisms, the uncertainties associated with the flux and energy values are arbitrarily taken as factors of 10 at the flux peak, and greater elsewhere; for the model, the lower limit is zero. The upper limit model flux and energy are independent of distance from Jupiter. These engineering models are based on the foregoing considerations, but should be considered extremely tentative.

In order to illustrate the possibly great range of proton flux values, figure 4 compares the above models with the limiting fluxes which can be trapped in Jupiter's magnetic field. The solid lines in the figure represent trapping limits, parametrized by proton kinetic energy E. The dashed lines represent the model fluxes of protons with E > 100 MeV. Although it has seldom been seriously proposed that the real flux values approach these trapping limits (see ref. 6), such fluxes are possible, do not violate any known observations or theoretical considerations, and would be severely hazardous if they were to reach spacecraft electronics.

CONCLUSIONS

Details of the engineering models for Jupiter's radiation belts based on the above considerations are presented in the Appendix. The magnetic field, securely based on the HF and UHF radio data, is strong and primarily dipolar, having field strengths near 14 G in the atmosphere, but it has few important impacts on spacecraft design directly. Although the dipole is nominally located at the center of Jupiter, it is inclined by about 10 deg and could be displaced up to 0.7 radii south of the center. The field is responsible for the containment of relativistic electrons, which are securely based on the UHF data. Their peak fluxes, near 10^7 cm^{-2} s^{-1}, and energies, near 6 MeV,

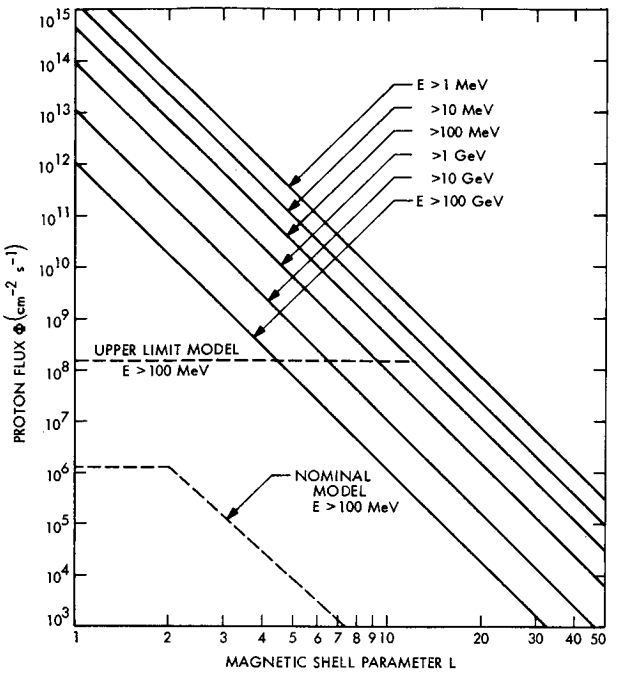

Figure 4. Flux Φ of energetic protons as a function of distance L from the dipole in the plane of the magnetic equator

could have some serious consequences for spacecraft design, particularly if their uncertain dependences of energy and flux far from the planet were relatively flat; nominally these dependences are expected to diminish rapidly with distance. The field may also contain energetic protons, for which apparently reasonable estimates and large uncertainties are presented. Even these values are severely hazardous for spacecraft electronics within two planetary radii of the dipole.

ACKNOWLEDGMENT

The assistance of Dr. James W. Warwick of the University of Colorado is gratefully acknowledged.

REFERENCES

1. Carr, T. D., and Gulkis, S.: The Magnetosphere of Jupiter, Annual Review of Astronomy and Astrophysics, vol. 7, 1969, p. 577.

2. Warwick, J. W.: Particles and Fields near Jupiter, NASA CR-1685, 1970, 123 pp.

3. Berge, G. L.: An Interferometric Study of Jupiter's Decimeter Radio Emission, Astrophys. J., vol. 146, 1966, p. 767.

4. Branson, N. J. B. A.: High Resolution Radio Observations of the Planet Jupiter, Monthly Notices of the Royal Astronomical Society, vol. 139, 1968, p. 155.

5. Anon.: 1970 October draft of "The Planet Jupiter (1970)," NASA Space Vehicle Design Criteria (Environments), to be published as NASA SP-80XX.

6. Luthey, J. L., and Beard, D. B.: The Electron Energy and Density Distribution in the Jovian Magnetosphere, Dept. of Physics and Astronomy, Univ. of Kansas, Lawrence, 1970, 19 pp.

7. Eggen, J. B.: The Trapped Radiation Zones of Jupiter, Report FZM-4789, Fort Worth Division, General Dynamics Corp., 1967, 44 pp.

8. Nakada, M. P., Dungey, J. W., and Hess, W. N.: On the Origin of Outer-Belt Protons, 1, J. Geophys. Res., vol. 70, 1965, p. 3529.

9. Gulkis, S.: Lunar Occultation Observations of Jupiter at 74 cm and 128 cm, Radio Science, vol. 5, 1970, p. 505.

10. Haffner, J. W.: Calculated Dose Rates in Jupiter's Van Allen Belts, AIAA J., vol. 7, 1969, p. 2305.

11. Koepp-Baker, N. B.: A Model of Jupiter's Trapped Radiation Belts, Report 68 SD 263, Missile and Space Division, General Electric Corp., 1968, 24 pp.

APPENDIX

Electron and proton concentrations and fluxes may be calculated from the formulas in table I for a specific position (specified by distance R and latitude ϕ with respect to Jupiter) and energy interval (between E and E + ΔE) according to the following procedure. Taking the radius of Jupiter as R_J = 71,422 km, calculate the magnetic shell parameter $L = R/R_J (\cos \phi)^2$. Evaluate the concentration parameter N_0 and the characteristic energy E_0 from two of the top eight formulas in table I, ignoring exponents following ± signs (use the pair appropriate to the particle kind, and appropriate for L less or greater than 2). Using the last formula in table I, calculate N_E, the particle concentration for energy greater than E, for both end points of the energy interval, and difference them (next-to-last formula in table I) to obtain $(\Delta E)_E$, the concentration in the energy interval of interest. Then apply the formula in the FLUX row to obtain the flux $(\Delta\Phi)_E$ in the interval; if (ΔE) is not much smaller than E, the procedure should be repeated with small intervals and the $(\Delta\Phi)_E$ values summed. Nominal interval concentrations and fluxes result, in which probably only two significant figures should be retained. Limiting ones are obtained in the same way, except that appropriate combinations of exponents following the ± signs in the expressions for N_0 and E_0 should be taken.

TABLE I. Formulas for trapped charged-particle radiation near Jupiter*

	Relativistic electrons	Energetic protons
Number density parameter for $0 \le L \le 2$	$N_0 = (6.3 \times 3^{\pm 1}) \times 10^{-4} \exp[-\phi^2/10^3]\,cm^{-3}$ (minimum $N_0 = 0$ for $0 \le L \le 1.6$)	$N_0 = (6.3 \times 10^{-4\pm 1}) \exp[-\phi^2/10^3]\,cm^{-3}$ (minimum $N_0 = 0$)
for $2 \le L \le 50$	$N_0 = \frac{5.8 \times 10^{-3}}{\exp[\phi^2/10^3]} \left(\frac{1.15}{L}\right)^{4\pm 2} cm^{-3}$	$N_0 = \frac{5.8 \times 10^{-3}}{\exp[\phi^2/10^3]} \left(\frac{1.15}{L}\right)^{4\pm 4} cm^{-3}$ (minimum $N_0 = 0$)
Characteristic energy for $0 \le L \le 2$	$E_0 = 6.2 \times 3^{\pm 1}$ MeV	$E_0 = 29 \times 10^{\pm 1}$ MeV
for $2 \le L \le 50$	$E_0 = 33\left(\frac{1.15}{L}\right)^{3\pm 2}$ MeV	$E_0 = 290\left(\frac{0.93}{L}\right)^{3\pm 3}$ MeV
Flux*† (interval distribution with energy) for $\Delta E \ll E$	$(\Delta\Phi)_E = c(\Delta N)_E$	$(\Delta\Phi)_E = c(\Delta N)_E \left\{\frac{\left[E\left(E + 2m_p c^2\right)\right]^{1/2}}{\left(E + m_p c^2\right)}\right\}$
Number density*† (interval and cumulative distributions with energy)	$(\Delta N)_E = N_E - N_{E+\Delta E}$ $N_E = N_0\left(1 + \frac{E}{E_0}\right)\exp\left(-\frac{E}{E_0}\right)$	

*For energies >1 MeV only.

†Table II gives $(\Delta N)_E$ and $(\Delta\Phi)_E$ as functions of E for $1.6 < L < 2$ and $\phi = 0$.

TABLE II. Energetic charged-particle concentrations and fluxes for individual energy intervals at the peak of Jupiter's trapped radiation belts ($1.6 < L < 2$ and $\phi = 0$)

Particle kind	Energy interval, MeV	Concentration $(\Delta N)_E$, cm^{-3}			Flux $(\Delta\phi)_E$, $cm^{-2}\,s^{-1}$		
		Minimum*	Nominal	Maximum*	Minimum*	Nominal	Maximum*
Electrons	1-3	2.2×10^{-6}	4.6×10^{-5}	6.4×10^{-4}	6.3×10^{4}	1.4×10^{6}	1.9×10^{7}
	3-10	1.9×10^{-5}	2.5×10^{-4}	1.1×10^{-3}	5.7×10^{5}	7.4×10^{6}	3.3×10^{7}
	10-30	9.8×10^{-6}	3.0×10^{-4}	1.0×10^{-3}	2.9×10^{5}	9.0×10^{6}	3.1×10^{7}
	30-100	0.0	2.9×10^{-5}	9.3×10^{-4}	0.0	8.7×10^{5}	2.8×10^{7}
	100-300	0.0	0.0	5.6×10^{-5}	0.0	0.0	1.7×10^{6}
	300-1000	0.0	0.0	0.0	0.0	0.0	0.0
Protons	1-3	0.0	2.8×10^{-6}	1.4×10^{-3}	0.0	5.6×10^{3}	2.9×10^{6}
	3-10	0.0	2.7×10^{-5}	3.7×10^{-3}	0.0	9.6×10^{4}	1.2×10^{7}
	10-30	0.0	1.4×10^{-4}	3.4×10^{-3}	0.0	8.8×10^{5}	2.0×10^{7}
	30-100	0.0	3.7×10^{-4}	3.7×10^{-3}	0.0	3.6×10^{6}	3.6×10^{7}
	100-300	0.0	8.9×10^{-5}	3.4×10^{-3}	0.0	1.3×10^{6}	5.5×10^{7}
	300-1000	0.0	0.0	3.7×10^{-3}	0.0	0.0	8.5×10^{7}
	1000-3000	0.0	0.0	8.9×10^{-4}	0.0	0.0	2.4×10^{7}
	3000-10,000	0.0	0.0	0.0	0.0	0.0	0.0

*Maximum (and Minimum) entries are interval-by-interval only, and do not yield a realistic cumulative spectrum when combined; to obtain the latter the formulas given in table I must be applied using specific values of N_0 and E_0.